Polypeptide–Metal Cluster Connectivities in Metallothionein 2 by Novel ^1H–^{113}Cd Heteronuclear Two-Dimensional NMR Experiments

Michael H. Frey,[†‡] Gerhard Wagner,*[†] Milan Vašák,[§] Ole W. Sørensen,[‡] David Neuhaus,[†] Erich Wörgötter,[†] Jeremias H. R. Kägi,[§] Richard R. Ernst,[‡] and Kurt Wüthrich[†]

Contribution from the Institut für Molekularbiologie und Biophysik, and the Laboratorium für Physikalische Chemie, Eidgenössische Technische Hochschule, 8093 Zürich, and the Biochemisches Institut, Universität, 8057 Zürich, Switzerland. *Received April 15, 1985*

Abstract: Two-dimensional heteronuclear ^1H–^{113}Cd and homonuclear ^{113}Cd–^{113}Cd correlated NMR spectra were recorded for ^{113}Cd–metallothionein 2 from rabbit liver. ^1H detection was used for the heteronuclear experiments. For 12 of the 20 cysteinyl residues, connectivities to one ^{113}Cd could be identified; for the other 8 cysteinyl residues, connectivities to 2 ^{113}Cd nuclei were detected ("bridging" cysteines). In combination with the independently obtained sequence-specific NMR assignments of the cysteine ^1H spin systems, the topology and the locations of the metal–sulfur clusters relative to the polypeptide structure could be established.

The elucidation of three-dimensional protein structures in solution by NMR[1] methods is in the process of becoming an established procedure in molecular biology.[2] The technique is particularly attractive for small proteins which are difficult to crystallize and to study with the use of X-ray crystallography. Metallothioneins belong to this class of proteins. They have been investigated extensively by a variety of chemical and physical methods,[3-8] but no crystal structure is yet available.

For most proteins, a structure determination by NMR will have to rely primarily on NOE observation of distance constraints between hydrogen atoms.[2] Metallothioneins, however, are of special interest because in addition to the spin $^1/_2$ nuclei ^1H, ^{13}C, and ^{15}N, which are ubiquitous in proteins, they may also contain spin $^1/_2$ metal ions, notably ^{113}Cd, which can be used for obtaining additional NMR constraints on the molecular conformation. To exploit these additional sources of structural information, novel heteronuclear 2D NMR experiments had to be devised. These are described in the present paper, together with the results obtained with their application to MT-2.

Figure 1 illustrates the impact of the data obtained with ^1H–^{113}Cd heteronuclear 2D NMR in the context of other studies using different NMR techniques. In its chemical structure, MT-2 consists of a polypeptide chain with 62 amino acid residues, including 20 cysteinyls and 7 divalent metal ions. The metal positions can be labeled for NMR studies by reconstitution of the protein with $^{113}Cd^{2+}$ (isotope enrichment >95%), without any major changes of the conformation as manifested in the ^1H NMR spectra. In the protein, the $^{113}Cd^{2+}$ ions are complexed exclusively via the sulfur of cysteine side chains (Figure 2A).[4-8] They show J couplings to the H^β signals in the Cys AMX spin systems,[9] but there is no evidence for direct J couplings between ^{113}Cd and H^α.[10,11] From general chemical knowledge, it can be inferred that the Cys sulfur may bind either to one or to two Cd^{2+} ions (binding to three metal ions seems also to be possible, but no evidence for such a type of ligation has been found in our data). Two ^{113}Cd nuclei attached to the same sulfur atom are expected to show a homonuclear scalar coupling.[7,8] The ^{113}Cd spectrum of MT-2 was first characterized by Armitage and co-workers[7,8] with one-dimensional NMR. Although their spectra contained more than the seven signals expected for seven metal binding sites, their homonuclear ^{113}Cd spin decoupling experiments indicated the existence of two metal thiolate clusters with three and four metal ions, respectively.[7,8] Later on Vasak et al.[12] and Dalgarno et al.[13] succeeded in getting ^{113}Cd-MT-2 preparations, showing just seven ^{113}Cd resonances, identical with those observed in this study (Figure 2B). Neuhaus et al.[10,11] identified the 20 cysteinyl ^1H spin systems from observation of the ^{113}Cd–^1H spin–spin couplings in the ^1H COSY spectra of MT-2, and the cysteines were arbitrarily labeled in the order of increasing H^α chemical shifts (Figure 1). Subsequently, sequence-specific assignments for all 20 cysteines were obtained[14] (Figure 1) with the use of

[†] Institut für Molekularbiologie und Biophysik.
[‡] Laboratorium für Physikalische Chemie.
[§] Biochemisches Institut.

(1) Abbreviations used: NMR, nuclear magnetic resonance; NOE nuclear Overhauser enhancement; COSY, two-dimensional correlated spectroscopy; NOESY, two-dimensional NOE spectroscopy; 1D, one-dimensional; 2D, two-dimensional; ppm, parts per million; J, spin–spin coupling constant; MT-2, metallothionein isoprotein 2 from rabbit liver; IUPAC-IUB one-letter symbols for amino acid residues with numbers are used to identify spin systems according to spectral parameters; three letter symbols with numbers are used to identify spin systems with the amino acid sequence position.

(2) (a) Wagner, G.; Kumar, Anil; Wüthrich, K. *Eur. J. Biochem.* **1981**, *114*, 375-384. (b) Wüthrich, K.; Wider, G.; Wagner, G.; Braun, W. *J. Mol. Biol.* **1982**, *155*, 311-319. (c) Braun, W.; Wider, G.; Lee, K. H.; Wüthrich, K. *J. Mol. Biol.* **1983**, *169*, 921-948. (d) Zuiderweg, E. R. P.; Kaptein, R.; Wüthrich, K. *Proc. Natl. Acad. Sci. U.S.A.* **1983**, *80*, 5837-5841. (e) Zuiderweg, E. R. P.; Billeter, M.; Boelens, R.; Scheek, R. M.; Wüthrich, K.; Kaptein, R. *FEBS Lett.* **1984**, *174*, 243-247. (f) Zuiderweg, E. R. P.,; Billeter, M.; Kaptein, R.; Boelens, R.; Scheek, R. M.; Wüthrich, K. In "Progress in Bioorganic Chemistry and Molecular Biology"; Ovchinnikov, Y. A., Ed.; Elsevier: New York, 1984; pp 65-70. (g) Wemmer, D.; Kallenbach, N. R. *Biochemistry* **1983**, *22*, 1901-1906. (h) Arseniev, A. S.; Kondakov, V. I.; Maiorov, V. N.; Bystrov, V. F. *FEBS Lett.* **1984**, *165*, 57-62. (i) Senn, H.; Billeter, M.; Wüthrich, K. *Eur. J. Biochem.* **1984**, *11*, 3-15. (k) Wüthrich, K.; Billeter, M.; Braun, W. *J. Mol. Biol.* **1984**, *180*, 715-740. (l) Williamson, M. P.; Marion, D.; Wüthrich, K. *J. Mol. Biol.* **1984**, *173*, 341-360. (m) Williamson, M. P.; Havel, T. F.; Wüthrich, K. *J. Mol. Biol.* **1985**, *182*, 295-315. (n) Kline, A.; Wüthrich, K. *J. Mol. Biol.* **1985**, *183*, 503-507.

(3) Nordberg, M.; Kojima, Y. In "Metallothionein"; Kägi, J. H. R., Nordberg, M., Eds.; Birkhäuser: Basel, 1979; pp 41-124.

(4) Vašák, M.; Kägi, J. H. R. In "Metal Ions in Biological Systems"; Sigel, H., Ed.; Marcel Dekker: New York, Basel, 1983; Vol. 15, pp 213-273.

(5) Vašák, M.; Kägi, J. H. R. *Proc. Natl. Acad. Sci. U.S.A.* **1981**, *78*, 6709-6713.

(6) Vašák, M.; Bauer, R. *J. Am. Chem. Soc.* **1982**, *104*, 3236-3238.

(7) (a) Otvos, J. D.; Armitage, I. M. *J. Am. Chem. Soc.* **1979**, *101*, 7734-7736. (b) Otvos, J. D.; Armitage, I. M. *Proc. Natl. Acad. Sci. U.S.A.* **1980**, 77, 7094-7098. (c) Boulanger, Y.; Armitage, I. M.; Miklossy, K.-A.; Winge, D. R. *J. Biol. Chem.* **1982**, *257*, 13717-13719.

(8) Armitage, I. M.; Otvos, J. D. In "Biological Magnetic Resonance"; Berliner, L. J., Reuben, J., Eds.; Plenum Press: New York, 1982; Vol. 4, pp 79-144.

(9) Wüthrich, K. "NMR in Biological Research: Peptides and Proteins"; North-Holland: Amsterdam, 1976.

(10) Neuhaus, D.; Wagner, G.; Vašák, M.; Kägi, J. H. R.; Wüthrich, K. *Eur. J. Biochem.* **1984**, *143*, 659-667.

(11) Neuhaus, D.; Wagner, G.; Vašák, M.; Kägi, J. H. R.; Wüthrich, K. *Eur. J. Biochem.* **1985**, *151*, 257-273.

(12) Vašák, M.; Hawkes, G. E.; Nicholson, J. K.; Sadler, P. J. *Biochemistry*, **1985**, *24*, 740-747.

(13) Dalgarno, D. C.; Armitage, I. M. *Adv. Inorg. Biochem.* **1984**, *6*, 113-138.

0002-7863/85/1507-6847$01.50/0

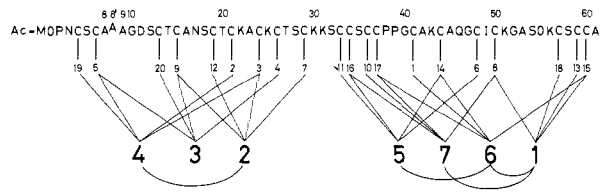

Figure 1. Survey of the chemical structure of rabbit liver metallothionein 2 and some salient NMR data on this protein. The top row presents the amino acid sequence as published[3] except that Asp10 was replaced by Gly, Gly11 by Asp, Thr17 by Asn, Lys20 by Thr, Ser39 by Pro, and an additional Ala was inserted between Ala8 and Ala9 (Ala8′). These changes were obtained from sequential resonance assignments[14] and are in agreement with recent chemical sequence analysis work (Hunziker, P.; Kägi, J. H. R., unpublished work). In the middle row, the AMX spin systems of the 20 cysteines are numbered according to the H^{α} chemical shifts[10,11] and at the bottom the 7 Cd^{2+} ions are numbered according to the ^{113}Cd chemical shifts (Figure 2B).[7,8] Straight lines show the ^{113}Cd–^{1}H spin–spin couplings identified in the present paper. Curved lines represent the ^{113}Cd–^{113}Cd couplings observed.

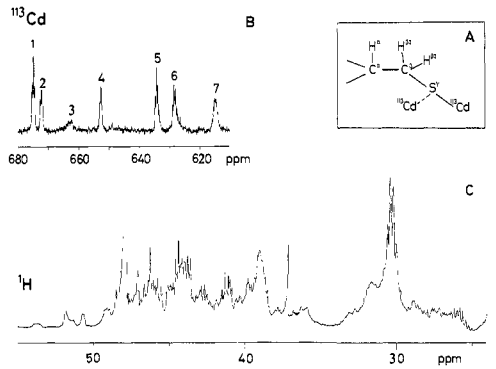

Figure 2. (A) Cysteine complexation with one or two $^{113}Cd^{2+}$ ions. The IUPAC-IUB atom notation is used. Since no stereospecific assignments were obtained for $H^{\beta 2}$ $H^{\beta 3}$, the ^{1}H NMR lines for these protons are identifed as $H^{\beta a}$ and $H^{\beta b}$, whereby $H^{\beta a}$ has the larger homonuclear spin–spin coupling constant $^{3}J_{\alpha\beta}$.[10]. (B) ^{1}H-decoupled 80-MHz 1D ^{113}Cd spectrum of MT-2. The signals are numbered 1 to 7 according to decreasing chemical shift. The chemical shift axis is calibrated relative to 0.1 M $^{113}Cd(ClO_4)_2$. (C) Region of the 360-MHz ^{1}H spectrum of MT-2 containing the H^{α} and H^{β} resonances of cysteines. The chemical shift axis is calibrated relative to internal sodium 3-(trimethylsilyl)-(2,2,3,3-$^{2}H_4$)propionate. Spectra (B) and (C) were recorded at 20 °C.

established procedures for the assignment of protein ^{1}H NMR spectra.[15,16] Combined with these ^{1}H NMR assignments, the ^{113}Cd–^{1}H heteronuclear correlation experiments described in this paper resulted in the identification of the Cd^{2+} coordination sites in the amino acid sequence (Figure 1). Furthermore, ^{113}Cd–^{113}Cd homonuclear COSY experiments enabled a check on the metal cluster architecture previously proposed based on different experiments.[7,8,17] It is readily apparent that the ensemble of ^{1}H–^{113}Cd and ^{113}Cd–^{113}Cd scalar couplings can be interpreted in terms of numerous distance constraints on the spatial folding of the polypeptide chain and on the relative spatial locations of polypeptide and metal ions. Combined with the ^{1}H–^{1}H NOE distance constraints, these data have already been used as input for the structure determination of MT-2 by distance geometry calculations,[18] and first results on the polypeptide fold of MT-2 have been obtained.[19]

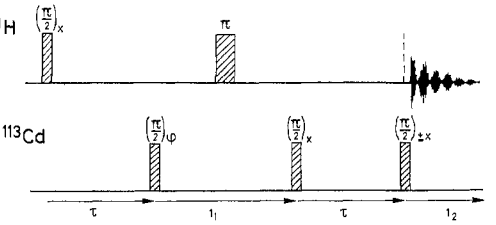

Figure 3. Pulse sequence for correlating ^{113}Cd with directly J-coupled protons (H^{β}) or coupling partners of the latter (H^{α}). The broken line in the ^{1}H channel represents either a z filter, a $(\pi/2)_y$ pulse, or a double-quantum filter (see text). The phase ϕ is cycled for the desired order p of ^{113}Cd coherence ($\phi = k\pi/p$, $k = 0, 1, ..., 2p - 1$, with alternated addition and subtraction of the free induction decays). Time proportional phase incrementation in steps of $\pi/2p$ along with t_1 can be added to distinguish positive and negative frequencies in ω_1.

Methods

^{113}Cd–^{113}Cd connectivities were determined by using a double-quantum-filtered COSY experiment[20] with gated broad-band ^{1}H decoupling during the evolution and detection periods. The chemical shifts along ω_1 were scaled by insertion of a 180° pulse in the evolution period at the time $\chi(t_1/2)$, with $0 < \chi < 1$.[21] The chemical shifts are thus reduced by the factor $(1 - \chi)$, whereas scalar couplings are not affected. This method can be applied in situations with well-separated cross peaks, which do not lead to overlaps even after chemical shift scaling. Longer t_1 increments can then be used, and with the same number of t_1 values, it becomes possible to expand t_{1max}, yielding improved resolution of multiplet patterns and less mutual cancellation of antiphase multiplet components.

For heteronuclear correlation experiments optimum sensitivity is achieved by employing indirect detection of ^{113}Cd. We used the basic pulse scheme described recently by Bax et al.[22a,b] and Bendall et al.[22c] (see Figure 3) with the modifications to be discussed below.

The experiment (Figure 3) involves creation of in-phase proton magnetization (represented by the operator I_{1y} in the product operator formalism[23]) by the initial ^{1}H $(\pi/2)$ pulse, which evolves during τ into coherence in antiphase with respect to the heteronuclear coupling $(2I_{1x}S_z)$. A ^{113}Cd $(\pi/2)$ pulse then transforms it into heteronuclear two-spin coherence[20] $(2I_{1x}S_y)$, which precesses during the evolution period, t_1. The ^{1}H π pulse in the middle of t_1 refocuses the heteronuclear J interactions and ensures that only the ^{113}Cd chemical shifts and the homonuclear couplings lead to modulations as a function of t_1. At the end of the evolution period, a second ^{113}Cd $(\pi/2)$ pulse transfers the two-spin coherence back to antiphase proton coherence $(2I_{1x}S_z)$, which then refocuses to in-phase coherence during the second τ delay.

The evolution of the magnetization under the proton–proton couplings during the second delay, τ, leads for fixed τ to peaks of variable phase. Incrementation of τ along with t_1 would lead to uniform phase but has the disadvantage of causing additional fine structure in ω_1 by the heteronuclear couplings in addition to the fine structure caused by ^{1}H–^{1}H couplings. We therefore chose to use fixed settings for τ and to apply purging procedures[20,23-26]

(14) Wagner, G.; Neuhaus, D.; Vašák, M.; Wörgötter, E.; Kägi, J. H. R.; Wüthrich, K. *Eur. J. Biochem.*, submitted.
(15) Billeter, M.; Braun, W.; Wüthrich, K. *J. Mol. Biol.* **1982**, *155*, 321–346.
(16) Wagner, G.; Wüthrich, K. *J. Mol. Biol.* **1982**, *155*, 347–366.
(17) Boulanger, Y.; Goodman, C. M.; Forte, C. P.; Fesik, S. W.; Armitage, I. M. *Proc. Natl. Acad. Sci. U.S.A.* **1983**, *80*, 1501–1505.
(18) (a) Havel, T.; Kunz, I. O.; Crippen, G. M. *Bull. Math. Biol.* **1983**, *45*, 665–720. (b) Braun, W.; Wider, G.; Lee, K. H.; Wüthrich, K. *J. Mol. Biol.* **1983**, *169*, 921–948. (c) Havel, T.; Wüthrich, K. *Bull. Math. Biol.* **1984**, *46*, 673–698.
(19) Braun, W.; Wagner, G.; Wörgötter, E.; Vašák, M.; Kägi, J. H. R.; Wüthrich, K. *J. Mol. Biol.*, in press.
(20) (a) Piantini, O. W.; Sørensen, O. W.; Ernst, R. R. *J. Am. Chem. Soc.* **1982**, *104*, 6800–6801. (b) Shaka, A. J.; Freeman, R. *J. Magn. Reson.* **1983**, *51*, 169–173. (c) Rance, M.; Sørensen, O. W.; Bodenhausen, G.; Wagner, G.; Ernst, R. R.; Wüthrich, K. *Biochem. Biophys. Res. Commun.* **1984**, *117*, 479–485.
(21) Brown, L. R. *J. Magn. Reson.* **1984**, *57*, 513–518.
(22) (a) Bax, A.; Griffey, R. H.; Hawkins, B. L. *J. Am. Chem. Soc.* **1983**, *105*, 7188–7190. (b) Bax, R. H.; Griffey, R. H.; Hawkins, B. L. *J. Magn. Reson.* **1983**, *55*, 301–315. (c) Bendall, M. R.; Pegg, D. T.; Doddrell, D. M. *J. Magn. Reson.* **1983**, *52*, 81–117.
(23) Sørensen, O. W.; Eich, G. W.; Levitt, M. H.; Bodenhausen, G.; Ernst, R. R. *Prog. NMR Spectrosc.* **1983**, *16*, 163–192.
(24) Sørensen, O. W.; Ernst, R. R. *J. Magn. Reson.* **1983**, *51*, 477–489.
(25) Sørensen, O. W.; Levitt, M. M.; Ernst, R. R. *J. Magn. Reson.* **1983**, *55*, 104–113.

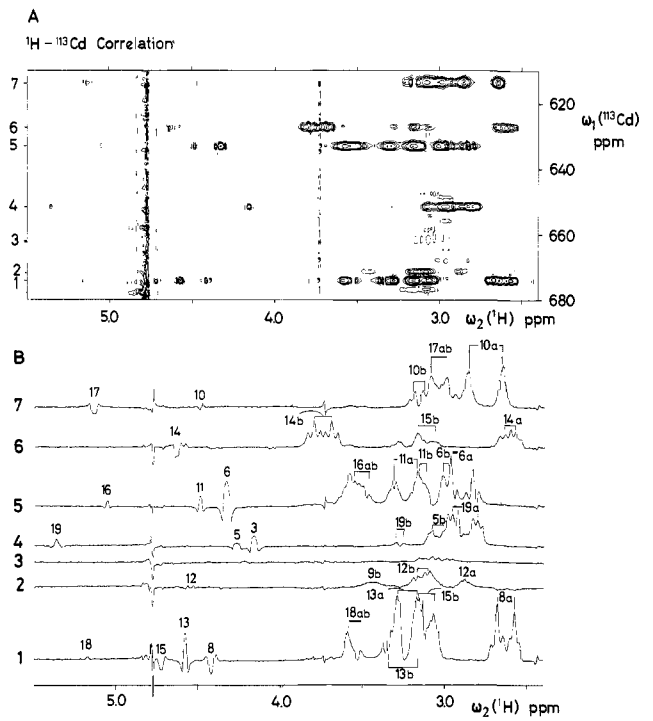

Figure 4. Heteronuclear ^1H–^{113}Cd COSY spectrum of MT-2 recorded with a z filter at the position of the broken line in Figure 3. The delay τ was 8 ms, the z filter delay was fixed at 2 ms, $T = 20$ °C. (A) Contour plot representation. The ^1H spectrum is along ω_2; the ^{113}Cd spectrum is along ω_1. The locations of the seven ^{113}Cd resonances are indicated on the left-hand side of the spectrum. Positive and negative levels are plotted without distinction. All cross peaks to H^β are in-phase absorptive along ω_1. (B) Cross sections along ω_2 at the ω_1 positions of the seven ^{113}Cd resonances as indicated on the left. H^β resonances of cysteines appear between 2.5 and 4.0 ppm, H^α resonances between 4.0 and 5.5 ppm. The cysteine signals are identified with arbitrary numbers according to the H^α chemical shifts (Figure 1)[10], where a and b indicate the H^β resonances with the larger and smaller coupling constant $^3J_{\alpha\beta}$, respectively.[10] The resonance splittings due to (^1H, ^{113}Cd) coupling are indicated with solid brackets. Any further splittings of the signals are due to (^1H,^1H) scalar coupling. The spurious signal at 4.78 ppm is due to the residual resonance of $^1H^2HO$.

prior to acquisition to obtain pure absorption profiles along ω_2. Absorption lines are advantageous for the measurement of $J(^{113}Cd, ^1H)$ or for identification of the cross peaks based on their characteristic (^{113}Cd,^1H) coupling constants which are known from analysis of ^1H–^1H COSY experiments of ^{113}Cd-MT-2.[10]

A first purging process is caused by the insertion of a phase-alternated ^{113}Cd $(\pi/2)$ pulse[24] prior to acquisition in Figure 3. It eliminates proton coherence in antiphase with respect to heteronuclear couplings. Alternatively, this could be achieved by ^{113}Cd decoupling during acquisition of the free induction decay. In addition, a z filter[23] $((\pi/2)_x-\tau_z-(\pi/2)_\xi)$ inserted at the position of the dotted line in Figure 3 eliminates the magnetization components in antiphase with respect to proton–proton couplings. A spectrum recorded with this purging scheme on the proton channel is shown in Figure 4. This pulse sequence has the advantage that the H^β resonances which are coupled to ^{113}Cd can be observed as in-phase absorptive signals. The splitting of the ^1H signals due to heteronuclear ^1H–^{113}Cd coupling can be identified by comparison with an experiment where ^{113}Cd decoupling during t_2 results in a collapse of the heteronuclear splitting (not shown).

Antiphase coherence caused by evolution under the ^1H–^1H couplings is transformed partially into two-spin coherence between H^α and H^β by the first $(\pi/2)$ pulse of the z filter. In case of incomplete τ_z averaging,[26] the second $(\pi/2)$ pulse of the z filter may lead to relay cross peaks between ^{113}Cd and the H^α of cysteine

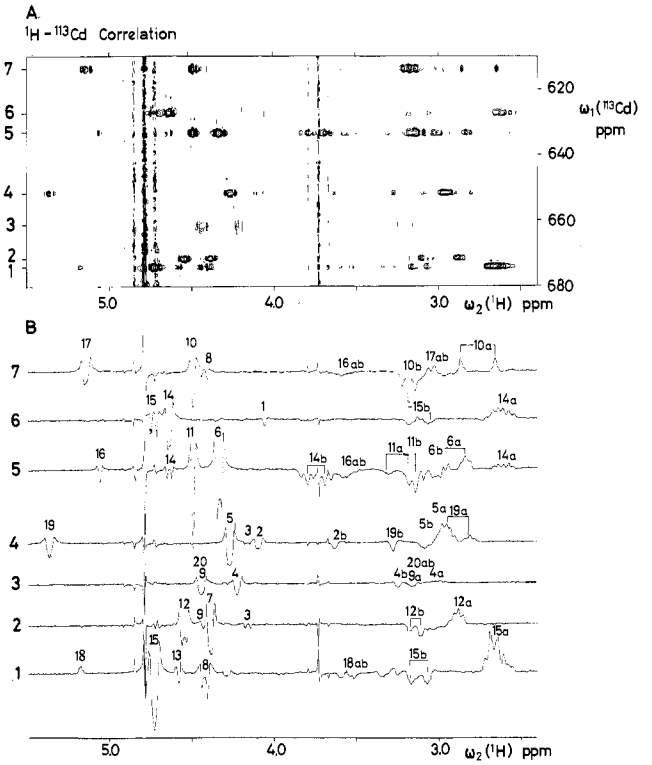

Figure 5. Heteronuclear ^1H–^{113}Cd COSY spectrum of MT-2. Same experiment as in Figure 4, except that the spectrum was recorded with a $(\pi/2)_y$ pulse at the position of the broken line in Figure 3 (see text). The delay τ was 30 ms.

(Figure 4). Because of the smaller number of H^α resonances, it is in practice often desirable to favor the Cd–H^α relay peaks at the expense of the Cd–H^β correlations. This can be done by placing a single $(\pi/2)_y$ relayed transfer pulse at the position of the dotted line in Figure 3. A spectrum obtained with this modified sequence is shown in Figure 5. When compared to Figure 4, the H^α signals are strongly enhanced. If simultaneous correlation of ^{113}Cd shifts with both H^α and H^β is desired, a proton double-quantum filter $((\pi/2)_x(\pi/2)_\psi)$ may be placed at the position of the dotted line. The double-quantum filter distributes the magnetization equally on the two positions and also acts as a phase-purging procedure.[20]

The intensity of the cross peaks in such experiments depends of course also on the length of the delay τ (Figure 3). The increased intensity of the remote peaks in Figure 5 compared to Figure 4 may therefore in part be due to the different τ values used. In order to obtain a complete set of connectivities, it is advisable to record several experiments with different τ values.

Experimental Section

^{113}Cd–^1H heteronuclear NMR spectra were measured on a Bruker AM-360 spectrometer, modified to allow ^1H observation at 360 MHz and ^{113}Cd pulsing at 80 MHz. Heteronuclear COSY experiments were recorded with the pulse scheme of Figure 3. Quadrature detection was used in both dimensions, and the carrier was placed in the center of the spectrum. Experiments with 128 t_1 values from 1 μs to 4.6 ms were recorded, each free induction decay consisting of 2048 data points, with an acquisition time of 0.45 s. Prior to Fourier transformation, the time domain data were multiplied with phase-shifted, squared sine bell window functions[27] with phase shifts of $\pi/4$ and $\pi/6$ in the ω_1 and ω_2 domains, respectively. The time domain data were extended to twice the original size by zero-filling in both the t_1 and t_2 directions, and a phase-sensitive Fourier transformation was carried out.

The homonuclear ^{113}Cd–^{113}Cd double-quantum-filtered COSY spectrum was recorded with 512 t_1 values from 4 μs to 72 ms. Each free induction decay consisted of 2048 data points, with an acquisition time of 0.14 s. Proton decoupling was performed during the t_1 and the t_2

(26) Sørensen, O. W.; Rance, M.; Ernst, R. R. *J. Magn. Reson.* **1984**, *56*, 527–534.

(27) Wagner, G.; Tschesche, H.; Wüthrich, K. *Eur. J. Biochem.* **1978**, *86*, 67–76.

periods. Prior to Fourier transformation, the time domain data were multiplied with phase-shifted sine bell window functions,[27] with phase shifts of $\pi/4$ and $\pi/6$ in the ω_1 and ω_2 directions, respectively. The further data handling was the same as for the heteronuclear COSY experiments.

MT-2 was prepared as described previously.[4-6] For the NMR measurements, ca. 0.01 M solutions of the protein in ^2H_2O, 0.02 M [$^2H_{11}$]-Tris/HCl, and 0.02 M KCl, p^{2}H 7.0 were used. All the measurements shown in the figures were carried out at 20 °C. Two further heteronuclear COSY experiments of the same type as shown in Figure 5 were carried out at 43 °C with delays τ of 50 and 60 ms, respectively. Sample tubes (5 mm) were used for the heteronuclear COSY experiments; a 10-mm sample tube was used for the homonuclear ^{113}Cd–^{113}Cd COSY experiment.

Results

For comparison, Figure 2 shows the part of the 1D ^{1}H spectrum containing the H$^\alpha$ and H$^\beta$ resonances of the cysteines[10] and the complete 1D ^{113}Cd spectrum. To record the ^{113}Cd spectrum, broad-band ^{1}H decoupling was applied during data acquisition. Seven ^{113}Cd resonances can be recognized[12] and are numbered according to decreasing chemical shift. The signals 2, 3 and 4 are less intense than the signals 1, 5, 6 and 7, probably because at pH 7 not all Cd^{2+} binding sites are equally populated. The resonance 3 is rather broad at 20 °C and sharpens at higher temperature, indicating an intramolecular-exchange process.

Connectivities between the signals of Figure 2B and C were obtained from the heteronuclear correlation experiments in Figures 4 and 5. Note that the heteronuclear COSY with ^{1}H detection has, besides the higher sensitivity, the advantage that the generally higher digital resolution along ω_2 can be utilized to resolve the crowded ^{1}H spectrum (Figure 2C). Figure 4A shows a contour plot of a ^{1}H–^{113}Cd correlation experiment, which emphasizes the direct Cd–H$^\beta$ connectivities (see Methods section). Figure 4B presents horizontal cross sections along ω_2 at the ω_1 positions of the seven ^{113}Cd resonances. H$^\beta$ signals occur upfield, H$^\alpha$ resonances downfield of 4 ppm.[10] In these cross sections, the H$^\beta$ resonances appear as in-phase absorptive and the H$^\alpha$ resonances as antiphase dispersive multiplets. In this spectrum, direct Cd–H$^\beta$ connectivities and remote connectivities to H$^\alpha$ signals were observed for 14 of the 20 cysteine spin systems. The assignment of the cross peaks to the well-resolved ^{113}Cd signals along ω_1 was straightforward. For the identification of the cysteine H$^\alpha$ and H$^\beta$ signals along ω_2, we relied on exact knowledge of the chemical shifts as well as the ^{1}H–^{1}H and ^{1}H–^{113}Cd coupling patterns obtained previously from ^{1}H–^{1}H COSY spectra.[10]

Difficulties in the analysis of the spectrum of Figure 4 arose both from the absence of the H$^\alpha$ cross peaks for six cysteines and from the poor separation of the signals in the H$^\beta$ spectral region. These limitations could be overcome by a modification of the heteronuclear COSY experiment which emphasizes the remote connectivities Cd–H$^\alpha$ (see Methods section). The result is shown in Figure 5. Cd–H$^\alpha$ cross peaks were observed for all 20 cysteines, and when previous knowledge on the Cys spin systems[10] was used, direct Cd–H$^\beta$ connectivities for 17 cysteines could also be established from this experiment. Six cysteines were identified as bridging cysteines from the experiments of Figures 4 and 5. Two additional experiments were recorded at 43° with τ values of 50 and 60 ms, respectively, with the same experimental scheme as in Figure 5. In these experiments, we identified another two bridging cysteines, yielding a total of 8 bridging and 12 singly bound cysteines. Two of the eight bridging cysteines, i.e., the cysteine spin systems C9 and C14, have been identified previously as bridging cysteines based on the multiplet structure of the (H$^\beta$,H$^\beta$) COSY cross peaks.[10]

Connectivies between the different ^{113}Cd signals were obtained from a homonuclear ^{113}Cd–^{113}Cd double-quantum-filtered COSY spectrum[17] (Figure 6). Four connectivities between ^{113}Cd spins which could be identified from this experiment are indicated in the figure.

Discussion

It has generally been accepted that MT-2 binds seven Cd^{2+} ions.[3,4,6-8] The presently used protein preparation gives indeed

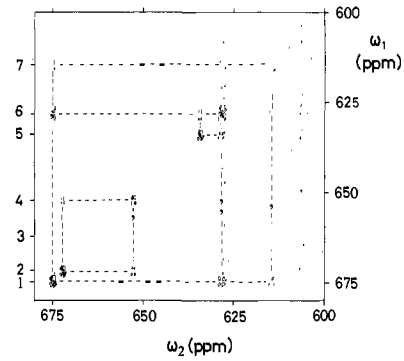

Figure 6. ^{113}Cd–^{113}Cd (80 MHz) double-quantum-filtered COSY spectrum of MT-2. The chemical shifts along ω_1 are scaled by a factor 0.5 as described in the text. The locations of the seven ^{113}Cd resonances are indicated on the left. Due to the ω_1 scaling, the multiplet structures appear elongated by a factor of 2 along ω_1. ^{113}Cd–^{113}Cd connectivities are indicated by broken lines.

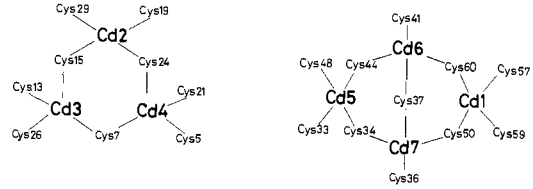

Figure 7. Structures for the two metal clusters in MT-2, which contain three and four Cd^{2+} ions, respectively, resulting from the heteronuclear ^{113}Cd–^{1}H connectivities (Figures 4 and 5) and the ^{113}Cd–^{113}Cd connectivities in Figure 6. The numbers of the cysteines refer to the positions in the amino acid sequence (Figure 1).

rise to seven resolved resonances[12,13] (Figure 2B). Two of these (5 and 6 in Figure 2B) have small shoulders on the high field side indicating the presence of small amounts (<20%) of a second MT species which is different from MT-1 and the major form of MT-2 (14). The occurrence of seven signals obviously implicates the existence of seven nonequivalent Cd^{2+} sites. The different intensities of the signals (Figure 2A), however, may correspond to different populations of these Cd^{2+} sites. Being aware of this, the following discussion examines the total number of connectivities to be expected for seven Cd^{2+} ions and compares these expectations with the number of experimentally observed cross peaks.

The Cd^{2+} ions of MT-2 are tetrahedrally coordinated,[4] and therefore each ^{113}Cd nucleus should show connectivities to four cysteine spin systems. This is indeed observed for all ^{113}Cd nuclei (Figure 1).

Identification of cysteines which bind two Cd ions (bridging cysteines) is of particular interest. While the original grouping of the seven Cd ions into two clusters was based on 1D ^{113}Cd spin-decoupling experiments,[7,8] the identification of "bridging" cysteines can also be used for distributing the Cd^{2+} ions to different clusters.[7,8,17] Since MT-2 contains seven Cd^{2+} ions which are bound to four sulfur atoms each, eight of the 20 cysteines must be bound to two Cd^{2+} ions.[4,6-8] Thus, each such pair of Cd^{2+} must be part of the same cluster. Six bridging cysteines can be identified unambiguously in Figures 3 and 4 based on the heteronuclear ^{113}Cd–^{1}H spin–spin couplings. Another two bridging cysteines were identified with analogous experiments at elevated temperature. Two of these eight spin systems have previously been identified as bridging cysteines on the basis of the multiplet structure of H$^\beta$–H$^\beta$ COSY cross peaks.[10] Independently, confirmation for the existence of four of these eight bridging cysteines was obtained from ^{113}Cd–^{113}Cd COSY cross peaks (Figure 6) since the geminal ^{113}Cd–^{113}Cd coupling is mediated via the thiolate sulfur atoms.

A survey of the results obtained from the present study combined with the sequence-specific assignments for the cysteines is given in Figure 1, and the resulting topology of the two metal clusters is shown in Figure 7. On the basis of the connectivities between Cd^{2+} ions and cysteinyl residues in specific locations in

the amino acid sequence, a rather detailed characterization of the metal cluster architecture was obtained. In particular, it is worth noting that two of the Cd^{2+} ions of the four-metal cluster, i.e., Cd1 and Cd7, are bound to cysteines in relative sequence positions $i,i+2$ and $i+3$. In further work on the structural interpretation of the present experimental data (Figure 1), the conformational constraints implied by the $^{113}Cd-^{1}H$ and $^{113}Cd-^{113}Cd$ scalar couplings are being used as input for the determination of the spatial structure of MT-2 with distance geometry calculations[18] in combination with $^{1}H-^{1}H$ NOE distance constraints and the complete, sequence-specific ^{1}H NMR assignments for the polypeptide chain.

Comparison of the presently obtained results (Figure 7) with the available literature shows on the one hand that the assignment of the $^{113}Cd^{2+}$ resonances to the two clusters and the $^{113}Cd-^{113}Cd$ connectivities within the clusters are consistent with the previous proposal made by Otvos and Armitage on the basis of 1D homonuclear ^{113}Cd decoupling experiments.[7,8] On the other hand, in a hypothetical model for MT-2 proposed by the same group[17] which included sequence-specific identification of the cysteines bound to the individual Cd^{2+} ions, 18 of the proposed 28 Cd-to-cysteine connectivities are incompatible with the present experiments, including all the proposed bridging cysteines.

After this manuscript was completed, we became aware that Otvos et al.[28] and Live et al.[29] applied 2D NMR experiments related to those in Figure 2 for studies of $^{113}Cd-^{1}H$ J connectivities in MT-2 and crab metallothionein, respectively. Their experimental schemes differ from those of Figure 3 by the absence of purging procedures. There are no obvious discrepancies between the $^{113}Cd-^{1}H$ couplings identified by Otvos et al.[28] and in the present paper. The comparison of the data is limited, however, since in those studies[28] the experiments were recorded at lower frequencies and the spectra were presented in the absolute value mode with reduced spectral resolution, and no resonance assignments other than the seven Cd were given.[30]

Acknowledgments. We thank M. Sutter for the preparation of the biological material and E. H. Hunziker and R. Marani for the careful preparation of the figures and the manuscript. This research was supported by the Kommission zur Förderung der wissenschaftlichen Forschung (Project 1120), the Schweizerischer Nationalfonds (Projects 3.284-82, 3.207-82, and 2.441-82), and the Science and Engineering Research Council (UK) (Overseas postdoctoral fellowship to D. N.).

Registry No. ^{113}Cd, 14336-66-4; Cd, 7440-43-9; Cys, 52-90-4.

(28) Otvos, J. D.; Engeseth, H. R.; Wehrli, S. *J. Magn. Reson.* **1985**, *61*, 579-584.

(29) Live, D.; Armitage, I. M.; Dalgarno, D. C.; Cowburn, D. *J. Am. Chem. Soc.* **1985**, *107*, 1775-1777.

(30) Note added in proof: After this paper was submitted, we were informed that a homologous metallothionein had been studied by crystallographic methods. The crystal structure of rat liver metallothionein isoform 2 has a substantially different arrangement of cysteines than reported here. The metallothionein in the crystals contains five Cd and two Zn per mole of protein (Melis, K. A.; Carter, D. C.; Stout, C. D.; Winge, D. R. *J. Biol. Chem.* **1983**, *258*, 6255-6257. Atomic coordinates for 414 atoms (61 amino acids, 7 metals) derived from a 2.3-Å resolution electron density map were deposited June 12, 1985 with the Protein Data Bank, Brookhaven National Laboratory, Upton, NY 11973 (Furey, W. F.; Robbins, A. H.; Clancy, L. L.; Winge, D. R.; Wang, B. C.; Stout, C. D.; manuscript in preparation).

Superdegenerate Electronic Energy Levels in Extended Structures

Timothy Hughbanks

Contribution from the Department of Chemistry, The University of Chicago, Chicago, Illinois 60637. *Received February 22, 1985*

Abstract: Near singularities may occur in the electronic density of states of crystalline compounds under circumstances described in this paper. Such "superdegeneracies" are described as they result from simple Hückel treatments of various systems. Although these superdegeneracies are accidental in that they are broken when interactions ignored in the simple Hückel model are restored, large peaks in the density of states remain. The concepts presented are applied to both real and hypothetical cases. Superdegenerate bands are shown to invariably have a nonbonding character which can be fully understood only by consideration of the orbitals available for bonding in the *extended structure*. While the bands which cause superdegeneracies are flat, the Wannier functions associated with these bands cannot be well localized. The physical implications of this poor localization are discussed. In cases where superdegenerate bands are half occupied, ferromagnetic ground states appear to be favored. Analogies to molecular cases, where the importance of localizability of Hückel nonbonding molecular orbitals has already been closely examined, may point the way for the extension of this work beyond the simple one-electron treatment given here.

In chemistry and physics, particular phenomena are described by theoretical models that are meant to serve as prototypes of real systems. The features of the models that are associated with these phenomena are often implicitly assumed to be necessary conditions for the occurrence of the phenomena in question. Such is the case in the explanation of narrow electronic energy bands and the concomitant peaks associated with these bands in crystalline solids. Narrow bands naturally arise when overlaps between atomic orbitals centered on neighboring atoms throughout a crystal are small. In the regime of small interatomic or intermolecular interaction, crystalline charge densities will differ little from those of the constituent atoms, molecules, or ions. The outgrowth of these observations is the assumption that narrow energy bands are to be found *only* when a system is characterized by at least one set of weakly interacting atomic or molecular orbitals. Simple physical prototypes in solid-state theory often ignore the kinds of subleties that specific structures may possess. This paper presents a discussion of cases in which flat bands are a consequence of the pseudo-symmetry of the extended structure of a solid *as a whole*. The underlying reasons for the occurrence of these highly degenerate bands are revealed by examining systems in the light of the simple Hückel model and its ability to uncover features that have a topological origin. The presentation is meant to be suggestive, and it is hoped that it will stimulate investigation into the ways in which particular extended structures show unusual properties because of these superdegenerate bands.

0002-7863/85/1507-6851$01.50/0